

RESEARCH ARTICLE

Polymer
COMPOSITES

WILEY

Mechanical and thermal properties of recycled polyethylene/surface treated hemp fiber bio-composites

Olcay Güney¹ | İbrahim Bilici² | Deniz Doğan³ | Ayşegül Ülkü Metin^{1,3}

¹Department of Defense Technologies, Kirikkale University, Institute of Science, Kirikkale, Turkey

²Department of Chemical Engineering, Hitit University, Faculty of Engineering, Çorum, Turkey

³Department of Chemistry, Kirikkale University, Faculty of Science, Kirikkale, Turkey

Correspondence

Ayşegül Ülkü Metin, Department of Defense Technologies, Kirikkale University, Institute of Science, Kirikkale, Turkey.

Email: aumetin@kku.edu.tr

Funding information

Kirikkale Üniversitesi, Grant/Award Number: 2021/021

Abstract

Hemp is a good option for polyethylene additives because of its high cellulose and fibrous content. This study aims to modify natural hemp fibers with the maleic anhydride/ionic liquid method, manufacture the composites, and compare the thermal and mechanical properties of natural hemp fiber and hemp cellulose. In this study recycled polyethylene as a binder, and filling ratios between 0 and 50 (wt/wt)% are investigated as a parameter. Differential scanning calorimeter and thermomechanical analysis were performed, and it was determined that the coefficient of thermal expansion from 973 to 147 ppm/K. It was determined that the strength of composite materials obtained from cellulose fibers with maleic anhydride/liquid ionic modification improved by around 20% from 19.5 to 24.4 MPa. In addition, as a result of scanning electron microscope analyses performed on the fractured surfaces, it was determined that the pressure, temperature, and time were suitable for producing composite materials. This work shows the potential of recycled polyethylene/hemp composites as a sustainable green material with simple fabrication procedure and useful mechanical and thermal properties.

KEYWORDS

cellulose, extraction, hemp fiber, ionic liquid modification, recycled polyethylene

Highlights

- Natural, cellulosic, and modified hemp fiber are used as a filler with different ratios.
- Recycled polyethylene used as a binder
- The liquid ionic modification increases the strength of recycled composites by up to 20%.
- Chosen pressure, temperature, and time were suitable for the production of composite
- Water absorption properties could be developed via modification.

This is an open access article under the terms of the [Creative Commons Attribution](https://creativecommons.org/licenses/by/4.0/) License, which permits use, distribution and reproduction in any medium, provided the original work is properly cited.

© 2023 The Authors. *Polymer Composites* published by Wiley Periodicals LLC on behalf of Society of Plastics Engineers.

1 | INTRODUCTION

Recently, with the effect of increasing environmental awareness and the desire to use natural resources more efficiently, there have been many researches on natural fibers instead of synthetic fibers.^{1–7} Besides the several benefits such as light weighting, low-processing costs, the research, and development of bio composites has another contribute to CO₂ sequestration.⁸

Hemp, is an appealing material for use as a filler in bio composites, as it is a plant with high mechanical properties, easy to grow, and has commercial value.^{6,9,10} It also has a relatively lower greenhouse effect and environmental impact after use than other synthetic materials.^{11,12} There are even studies where hemp residues can inhibit soil nematodes, pathogenic fungi, botanical insecticides, or miticides.¹³ It has been used as a filler in composite materials due to its fiber structure and mentioned properties. Studies have shown no significant change in the crystalline content after recycling. In this respect, it is a plant with a high probability of being reused.¹⁴ Mechanical properties are at the forefront of the parameters studied about hemp in composite materials. In these studies, mostly mechanical properties such as impact, shear stress, and tensile stress was analyzed and investigate with the different binders.^{15,16} The studies of various binders has been reported such as biodegradable polymers,¹⁷ polyethylene,¹⁸ epoxies,^{19,20} polypropylene,^{21–23} polybutylene adipate-co-terephthalate,²⁴ polyamide PA 11,²⁵ and so forth. In most of the studies, different compatibilizers and plasticizers were used to improve the mechanical properties of binders.^{17,26} The use of compatibilizers is significantly interesting because hemp consists of crystalline cellulose (55%–72%), lignin (2%–5%), hemicellulose (8%–19%), and lesser amounts of waxy compounds, which can be modified to enhance interfacial bonding.

Treatments on hemp fiber could be different methods such as removing non-fiber components, surface treatment, and reducing the hydrophilicity for better interaction with the binder. For this reason, many other treatment methods, such as enzymatic treatment,²⁷ steam explosion and plasma treatment,²⁸ alkali treatment,^{29–31} and silane treatment,³⁰ are used in the literature. To reduce environmental concerns associated with the end of life of post-consumer plastics, recycling is a one of the best action. The root cause for choosing polyethylene is the thermal properties of recycled polyethylene are very close to virgin and one of the most post-consumer plastic materials^{32,33} in the world. In addition, most of the existing polyethylene waste is still landfilled.³⁴ Therefore, increasing the usage areas of recycled polyethylene will contribute positively to reducing greenhouse gas emissions and preventing microplastic formation.³⁵

This study aims to investigate the production of a polymer-based green composite consisting of recycled polyethylene and cellulose fibers, which are extracted hemp fibers as a sustainable reinforcing material. The cellulose fibers were modified via the ionic liquid method by maleic anhydride (MA) to improve the matrix-fiber interaction. The effectiveness of the cellulose extraction process and liquid ionic modification method was evaluated by x-ray diffraction (XRD), thermogravimetric analysis-differential thermal analysis (TGA/DTG), differential scanning calorimetry (DSC), and Fourier transform infrared spectroscopy (FTIR) characterization, as well as MFI, hardness mechanical, and thermomechanical properties.

2 | METHODOLOGY

2.1 | Chemicals

Recycled-polyethylene (rPE, melting point: 128°C; melting flow index: 0.4987 g/min) was purchased from Guangzhou Lushan Nem Materials Co. MA, and 1-butyl 3-methyl imidazolium chloride (BMIC) was purchased from Sigma-Aldrich. Hemp plants were obtained from the Central Anatolian Region of Turkey.

2.2 | Extraction of cellulose from hemp fibers

Full-length stripped form hemp fibers were obtained from the hemp plant to be used in the study. The hemp fibers were cut about 1 cm long. After being washed with distilled water and dried, it was pulverized in a Wiley mill. Samples passed through an 80 µm sieve were used. These fibers were abbreviated as raw hemp (NF) in the following sections. Cellulose extraction was carried out in three stages with minor modifications to the methods defined in the literature.^{30–32} First, the bleaching of NF by treating with H₂O₂ (7% vol/vol) and NaOH (4% wt/vol) (1:1 vol/vol) solution in a water bath at 60°C for 3 h^{36,37} was performed. In the second stage, the H₂SO₄ solution was in different concentrations (5%–30% (vol/vol), 50 mL) with bleached fibers at 60°C for 3 h. The concentration of H₂SO₄ solution selected for this study was based on previous researches^{38–40} treated. The cellulosic fibers were washed with deionized water and dried in an oven at 40°C. The effect of H₂SO₄ concentration on the chemical extraction process was determined by XRD analysis. Cellulosic nanofibers obtained under the determined optimum conditions were used in the next stage of the study and abbreviated as CNF.

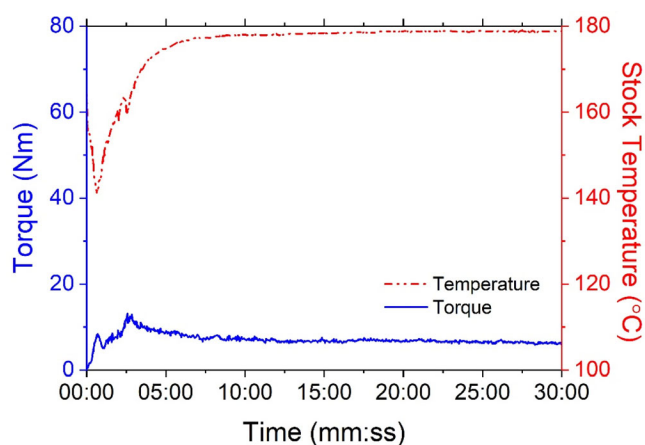


FIGURE 1 Plastogram of recycled-polyethylene (rPE) composites.

2.3 | Surface modification of cellulosic fibers with MA

For MA modification, dried cellulosic nanofibers were refluxed at 110°C for 10 min in 1-butyl 3-methyl imidazolium chloride solution (5% (wt/vol)) prepared with dimethyl sulfoxide.⁴¹ Then, the MA solution (20 mL, CNF: MA = 1:0.5) dissolved in propanol was slowly added to the reaction medium. The modification reaction was carried out at 110°C for 10 h. At the end of the reaction, MA-modified cellulosic nanofibers (CNF_MA) removed from the environment were washed with distilled water and dried in an oven at 40°C.

2.4 | Bio-composites preparation and processing

In the first stage of producing raw hemp, cellulosic nanofiber and MA-modified cellulosic fiber-reinforced recycled polyethylene matrix composite materials, fiber, and polymer were mixed using a Brabender/W50 EHT + Plastograph EC Plus to form a homogeneous structure. The mass ratio of reinforcing elements in polymer matrix composite materials was prepared in the 5%–50% range. For this purpose, the fibers were mixed with rPE set at 175°C for 30 min and 50 rpm. As can be seen from the plastogram in Figure 1, the mixture became homogeneous after 8 min. The stirring was continued for 30 min to be sure. Although the temperature is set to 175°C, the actual temperature is around 178–179°C. The resulting mixture was granulated in a 6 mm sieve-size crusher and molded in a mini-injection molding device with a temperature of 175°C and a pressure of 800 bar, following ISO 527-2-5A standards.

2.5 | Instrumentation

The morphology and characteristics of fibers were analyzed using scanning electron microscopy (SEM), XRD, thermogravimetry, and FTIR.

The functional groups of the fibers were identified using FTIS (Bruker Vertex 70 V model FTIR Spectrometer with ATR modulus) in the range of 400–4000 cm^{-1} at number of 32 scan. After extraction, cellulosic fibers' surface charge and size distribution were determined using Zetasizer (Malvern-Nano ZS). XRD analysis was performed by Rigaku Ultima IV diffractometer with Cu $K\alpha$ radiation (40 kV, 40 mA) in the range of 0°–90° at a scanning rate of 1° min^{-1} . Then empirical method was used to obtain the crystallinity index of the samples X_c , as shown in Equation (1)⁴³:

$$X_c = I_{200} - I_{am} / I_{200} \times 100 \quad (1)$$

where the I_{200} represents the maximum density of the peak at 2θ between 22.5 and 22.6° and I_{am} corresponds to about $2\theta = 18^\circ$.^{36,42}

The morphological properties of raw hemp fibers and cellulosic nanofibers were determined using SEM (Carl Zeiss/Gemini 300) by gold coating under 15 kV voltage. RPE/hemp's surface morphology is also observed under 5–10 kV voltage using a SEM (JEOL 5060). Thermal stability of the fibers was determined in the range of 25–900°C using a TGA instrument (Perkin Elmer Pyris) at a 10°C/min heating rate under N_2 . Thermomechanical properties were determined using a thermomechanical analysis (TMA; Mettler-Toledo, SDTA 841) under a 0.5 N constant load and at 110°C. The thermal properties of hemp fibers, RPE, and RPE/hemp composites were determined using DSC (Mettler-Toledo/DSC 1/700) in a nitrogen atmosphere, with a rising rate of 10°C min^{-1} and a temperature range of 25°C. The hardness values of rPE/hemp composite materials were determined using Mitutoyo Hardmatic Type A/Type D hardness, and tensile strengths were determined with Shimadzu AG-I /5 kN tensile device using five samples according to ISO 527-2-5a standard. The mixture of fiber and RPE was prepared using a laboratory-type plastic injection device (Thermo Scientific HAAKE Minijet II), using molds conforming to ISO 527-2-5a standards. The melt flow index (MFI) of RPE-based composites was determined at 230°C using the Instron/Ceast MF20.

The composite samples with dimensions 50-mm long, 10-mm wide, and 3-mm thick were dried until constant weights were achieved. They were then immersed in distilled water at room temperature for 14 days. At the pre-determined interval, specimens were removed, dried,

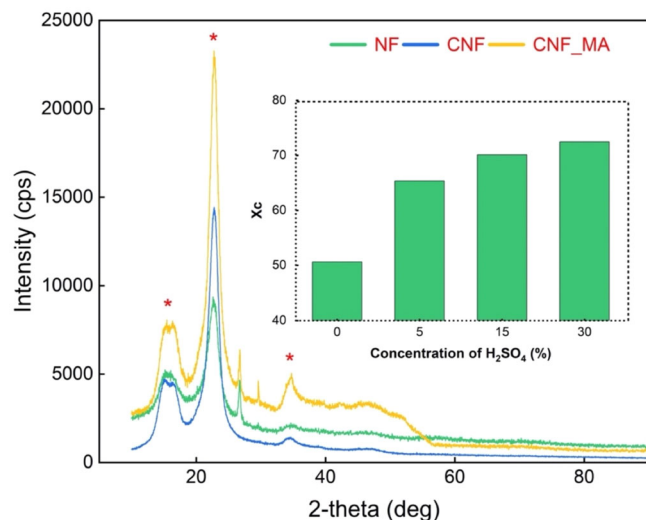


FIGURE 2 X-ray diffraction patterns of raw hemp (NF), cellulose (CNF), and maleic anhydride-modified cellulose (CNF_MA).

weighed, and returned to the water. Water absorption capacity was calculated according to Equation (2).

$$\% \text{water absorption} = (m_w - m_d / m_d) \times 100 \quad (2)$$

where m_w is the wet weight of the samples and m_d is the dried weight of the sample.

3 | RESULTS AND DISCUSSION

3.1 | Characterization studies of raw hemp, cellulose, and MA-modified cellulose

3.1.1 | XRD studies

The effect of H_2SO_4 concentration on the cellulose extraction efficiency was evaluated using XRD analysis. For this purpose, the crystallinity index value (X_c) was calculated using the formula proposed by Segal et al., as given in Equation (1)⁴³:

As seen from the XRD patterns, the peaks at the $2\theta = 16.8^\circ$ and 22.86° peaks representing the typical cellulose I structure and crystal integrity are preserved in the diffraction patterns of all samples (Figure 2). Cellulose I typically have well-defined three peaks in a diffraction pattern of $2\theta = 16^\circ$, 22° , and 35° , and no double peaks were observed at $\sim 2\theta = 22^\circ$.⁴⁴ As a result, according to the XRD diffraction pattern, it was determined that the cellulose fibers preserved their crystalline structure with the applied chemical treatment, while the crystallinity

value increased with the chemical treatment.⁴⁵ According to the calculated X_c values, the crystallinity of raw hemp fibers increased after the extraction process. While the crystallinity index value for the raw hemp was 50.61%, it increased depending on the H_2SO_4 concentration used. While the X_c value was $\sim 65\%$ at 5% of the H_2SO_4 solution, it reached $\sim 72.47\%$ after extraction with 30% of the H_2SO_4 solution (Figure 2). The crystallinity index increases due to the removal of hemicellulose, lignin, and amorphous polymers from the plant structure. However, similar to cellulose, MA-modified cellulosic nanofibers show typical peaks of cellulose at $2\theta = 16.94^\circ$, 22.7° , and 35° . In addition, due to MA modification, distinct new peaks were formed in the diffraction pattern of cellulose at $\sim 2\theta = 26.6^\circ$ and 29.66° . The peaks formed were thought to belong to 1-butyl 3-methyl imidazolium chloride used in MA modification.⁴⁶ In addition, the X_c value for CNF_MA cellulosic fibers was calculated as 65.36%.

3.1.2 | FTIR studies

Hemp fiber is mainly composed of cellulose, hemicellulose, and lignin. Cellulose constitutes $\sim 75\%$ of the total mass of hemp fiber.^{47,48} The residual components are pectin, lignin, vegetable waxes and oils, water-soluble substances, and moisture.⁴⁹ Depending on the presence of chromophore groups in the lignin structure, the fiber color changed after the applied chemical treatment steps.^{50,51} As seen in Figure 3, the white color of the hemp fibers after chemical extraction indicates that colored groups, such as lignin, have been removed from the structure. However, the yellow color of the fiber after the reaction with MA represents that the modification process has taken place successfully.

FTIR spectroscopy was used to detect changes in the chemical structure of raw hemp during the extraction process (Figure 3). In the untreated and extracted fibrils, a wide absorption band between 3300 and 3500 cm^{-1} corresponding to stretching vibrations of the free $-\text{OH}$ groups in cellulose were recorded.^{52–54} The increase in the intensity of this band indicates an increase in cellulose content due to the removal of the lignin after chemical treatments.⁵⁵ The bands at about 2900 cm^{-1} belong to stretching vibration of methyl and methylene groups. After extraction, the increase in the intensity and width of the peak observed in this region is significant. $\text{C}-\text{O}$ stretching vibration, $\text{C}-\text{O}-\text{C}$ asymmetric stretching vibration, and $\text{C}-\text{H}$ vibration of the cellulose structure are observed at 1022, 1124, and 1386 cm^{-1} , respectively.³⁶ Also, the bands observed at 895 and 1720 cm^{-1} belong to cellulose's characteristic

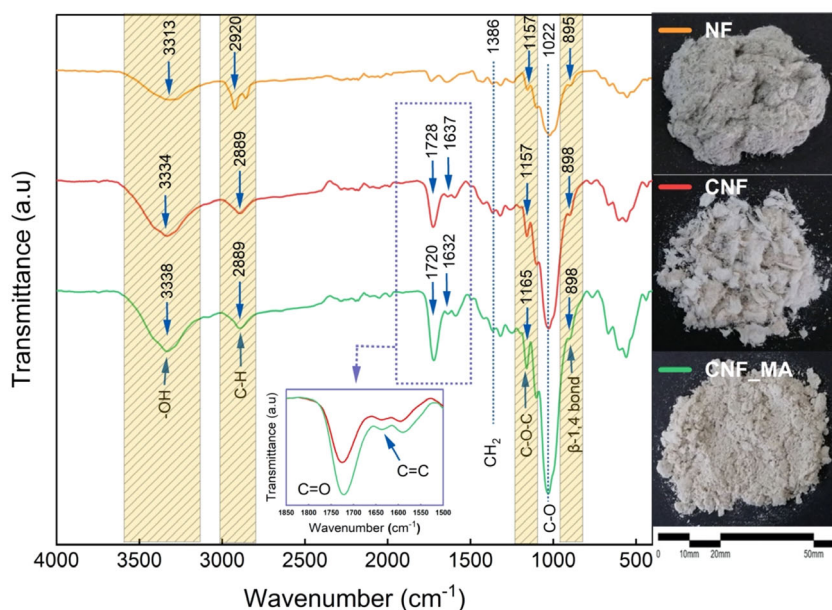


FIGURE 3 Fourier transform infrared (FTIR) spectra of raw hemp (NF), cellulose (CNF), and maleic anhydride modified-cellulose (CNF_MA).

β -glycosidic bond and carbonyl groups (C=O) in cellulose, respectively. As a result, strong absorption bands in cellulose are consistent with cellulose's characteristic bands.

In the FTIR spectrum of CNF_MA fibers, the increase in the carboxyl tensile band at 1720 cm^{-1} , and the bands of vinyl groups (C=C) at 1632 cm^{-1} indicate that the malonyl group binds to cellulosic nanofibers and MA modification occurs successfully.^{41,56–58}

3.1.3 | Morphological properties

Figure 4 shows micrographs of the surface of raw hemp (A), the surface and cross-section of cellulosic nanofibers (B-I and B-II), and the cross-section of cellulose at the end of MA modification. It was determined that after acid extraction in raw hemp fibers, fiber bundles were opened due to the removal of hemicellulose, lignin, and other impurities on the fiber structure. It was like a sheet (B-I). When the vertical section view was evaluated, it was seen that the bundle state of the cellulosic nanofibers decreased, and the filaments opened after the MA modification (B-II and B-III). SEM analysis are showed the treatment of hemp with a Maleic Anhydride has removed impurities from hemp surface and also could led to poor stress transfer subsequently caused to low mechanical properties. In addition, it is evaluated that the heterogeneous surface area of this more irregular and rougher surface, which is thought to be caused by the modification, will increase the specific surface area of CNF_MA and its interaction with the polymer.⁵⁷

3.1.4 | Thermal properties

Figure 5 shows the thermal degradation (TGA), derived thermal degradation curves (DTG), and DSC curves of NF, CNF, and CNF_MA nanofibers. Removal of moisture or volatile compounds (mass loss of 10%) occurs in the temperature range of up to 100°C . Due to differences in their chemical structures, hemicellulose, cellulose, and lignin generally decompose at different temperatures.⁵⁹ There was a sharp weight loss at about 338°C for NF, while for CNF fibers, this mass loss was observed at 385°C . It is thought that this is due to the removal of amorphous regions such as lignin and hemicellulose in the structure of raw hemp. This variation in decomposition temperatures is seen more precisely than the DTG curves. For raw hemp fibers, the DTG peak appears to occur at lower temperatures than for chemically extracted hemp fibers. However, the shoulder observed in the DTG curve of raw hemp fiber at low temperatures is attributed to hemicellulose, which degraded earlier.⁶⁰

So far, cellulosic nanofibers have been obtained by chemical extraction from different plant species, with similar results achieved above. Karzadeh et al. compared the thermal behavior of cellulose nanocrystals extracted from kenaf fiber by H_2SO_4 acid hydrolysis. It was determined that the decomposition temperature of 328°C increased to 350°C for cellulose nanocrystals, and the applied process increased the thermal stability of the fibers.⁶¹ Our previous study, which extracted Cellulose from *Phragmites australis*, stated that the degradation temperature of the *P. australis* increased to 351°C after the extraction process.³⁶ On the other hand, the thermal stability of CNF fibers decreases after MA surface

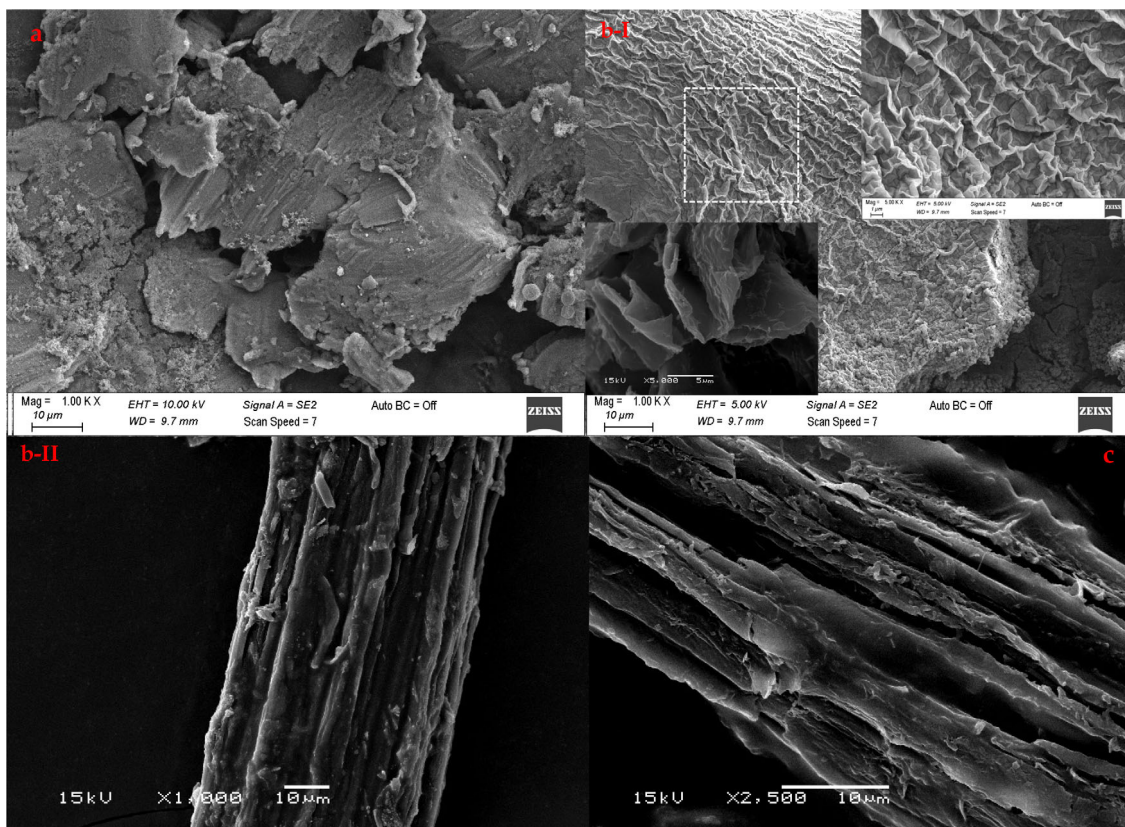


FIGURE 4 Scanning electron microscope (SEM) micrographs of raw hemp (A), surface (B-I), and vertical section (B-II) of cellulose and maleic anhydride-modified cellulose (C).

treatment. The temperatures at which CNF and CNF_MA nanofibers lost 50% of their mass were determined as 375.98 and 358.37°C, respectively. The reduction in thermal stability also confirms the decrease in X_c values calculated from XRD patterns. Modifying CNF nanofibers with MA reduced the crystallinity and, thus, the thermal stability of nanofibers. It can be due to weaken the strong intermolecular hydrogen bonds established between the cellulose chains and provide tight stacking with the modification. In previous studies, it has been reported that as the amount of hydrogen bonding between cellulose chains increases, the chains get closer to each other, and the thermal stability of the molecule increases with increasing crystallinity. Accordingly, a study comparing cellulose fibers obtained from different plant species reported that the thermal stability of *Dipteryx odorata* and *curaua* fibers was relatively high.⁶²

Figure 5 also shows the DSC curves of all cellulose samples. The first endothermic peaks in the 60–70°C range can be due to the removal of water and volatile organic molecules from the structure. While this temperature was 70°C for cellulose fibrils, it shifted to 60.8°C for MA-treated fibers. A similar observation has previously been reported. Cichosz et al. noted the chemical

modification of ultrathin cellulose for paper and cardboard coatings with vinyltrimethoxysilane and MA.⁶³ However, the melting peaks of the fibers, while it was 351°C for cellulose nanofibers, decreased to 298°C after MA modification, which is compatible with TGA analysis. Finally, after the modification process, the thermal stability of the cellulose nanofibers decreased.

3.2 | Characterization studies of rPE-based bio-composites

3.2.1 | DSC analysis of composites

DSC thermograms of recycled polyethylene and manufactured composite materials are given in Figure 6. In the calculations made using the Star-e software, the melting point was determined to be ~128°C. This shows that the amount of high-density polyethylene (HDPE) is high in recycled polyethylene. One of the main reasons why the peaks here fluctuate between 123 and 128°C is the impurity of the binder material used. The very few samples used due to the nature of DSC analysis can also be considered as a factor. Therefore, fluctuations around

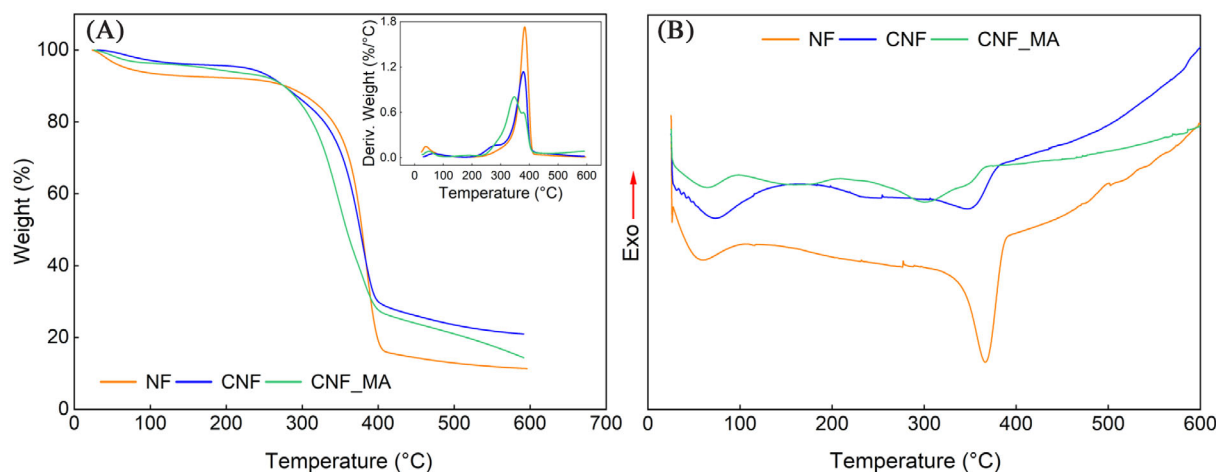


FIGURE 5 (A) Thermogravimetric analysis-differential thermal analysis (TGA/DTG) thermograms and (B) differential scanning calorimeter (DSC) curves of nanofiber (NF), cellulosic NF (CNF), and CNF_MA fibrils.

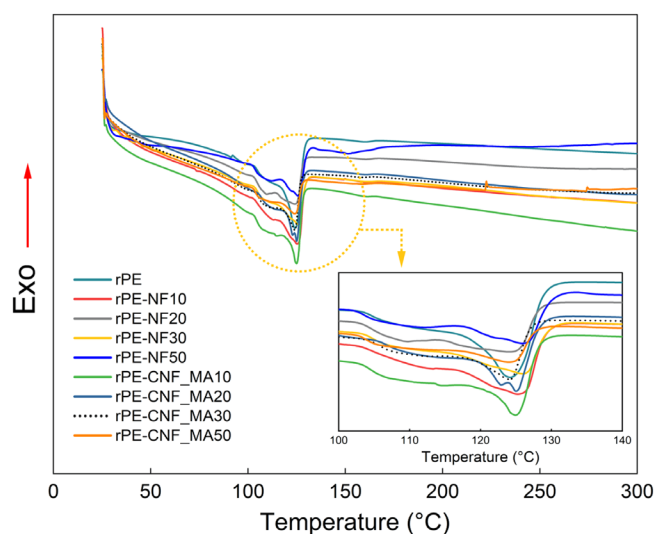


FIGURE 6 Differential scanning calorimeter (DSC) thermograms of recycled-polyethylene-nanofiber (rPE-NF) and rPE-CNF_MA composites.

melting peaks can be characterized as impurities and can be neglected.

In detail given in Figure 6, it is seen that the melting point peak changes with the change of the additive. The main point, when NF, CNF, and CNF_MA in Figure 5B are compared with up to 300°C, it is seen that the strong endothermic peak in these ranges is generally caused by rPE. With the change of additive content, there is little change in melting temperatures among themselves. The main point can be attributed to the heterogeneous crystallization on the surface of NF and CNF, which can improve the crystallization of recycled PE, then slightly increase the melting temperature of rPE composites.⁶⁴

3.2.2 | Thermomechanical analysis

Coefficient of thermal expansion (CTE) is a material property that is indicative of the extent to which a material expands upon heating. Depending on the material type, these expansions may vary for each temperature. In small temperature ranges, this ratio is proportional to the temperature change. With respect to temperature, the magnitude of CTE increases with increasing temperature. While these ratios are low in ceramic materials, they generally increase in metals and polymers, respectively. TMA results are given in Figure 7 and Table 1. With the increase in temperature, rPE showed a shrinkage of about 2.1%. With the increase in NF, this decreased to about 0.50%. The shrinkage ratios of rPE-CNF composites decreased to 0.4% after 50% cellulosic nanofiber additive (Figure 7). As cellulosic nanofiber's additive ratio increases, 20% more dimensional stability is achieved than raw hemp fibers. This situation increases the thermal stability of the composite material by providing a better fiber-matrix interface by removing the amorphous regions from the structure of the cellulosic nanofibers obtained by the extraction process from raw hemp. Similar observations were obtained with the composites prepared with MA-modified fibers, and almost no change was observed in the dimensions of the composite with 50% fiber reinforcement.

Table 1 shows the variation in the CTE of rPE depending on all cellulose types and additive ratios. In general, it has been stated that with the increase of the reinforcement ratio in composites, swelling due to the trapped moisture in the composite and expansion, as a result, will occur.⁶⁵ However, the thermal expansion coefficient of the produced composites is lower than that of rPE. This result suggests that the

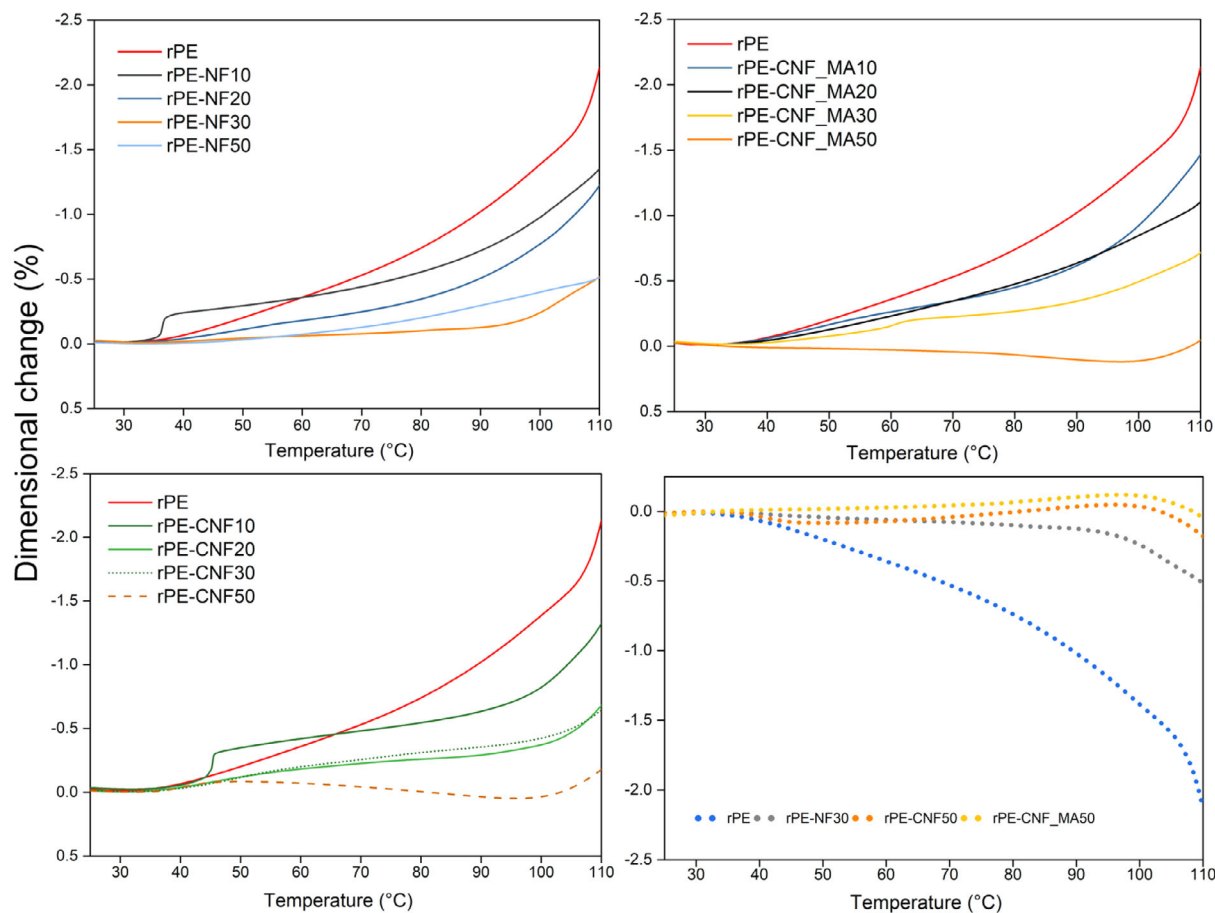


FIGURE 7 Effect of temperature on dimensional changes of recycled-polyethylene (rPE)-based biocomposites.

composite does not contain trapped air or moisture, indicating the suitability of process parameters such as pressure, temperature, and time applied during production.

The thermal expansion coefficients of rPE-CNF composites were similar to NF, and it was observed that the thermal expansion coefficients of the rPE-CNF composites decreased with the increase in the additive ratio. When the dimensional changes and thermal expansion coefficients were evaluated together, it was assessed that the optimum additive ratio was 30% for NF and CNF fibers. Similar results were observed with composites prepared with MA-modified fibers. Almost no change was observed in the dimensions of the composite with 50% fiber reinforcement. While this type of composites produced by injection is cooled from the molten state to ambient temperature, it changes state faster than reaching thermodynamic equilibrium. As seen in the data given in Table 1, this expansion in rPE is higher at high temperatures than all additive ratios. This shows that modified composites will provide great convenience in production techniques.

3.2.3 | Melt flow index

The MFI is one of the critical parameters used to determine the flow properties of polymer materials during the production phase. Figure 8 shows that the MFIs recorded for all composite types decrease as the cellulose fiber content increases. The viscosity and melting stability of the polymer increased; that is, the MFI value decreased as the reinforcement ratio increased in all three reinforcement types. The MFI values of rPE-NF, rPE-CNF, and rPE-CNF_MA composites decreased by ~90%–98%, 88%–94%, and 87%–92%, respectively, compared to pure rPE (4.987 g/10 min). This behavior is mainly due to the relatively stiff and rigid fibers used as reinforcement, which hinder the rearrangement of polymeric chain segments, disturbing their movement into the melt and increasing their melting viscosity.

The decrease in MFI values is due to the reinforcement of the hemp fiber, moving to the polymer chains complex, and the flow ability of the composite decreased.⁶⁶ Many studies recorded the change in MFI values of polymer composites. For example, a decrease in MFI values with cellulose reinforcement in LDPE

TABLE 1 Thermal expansion coefficients of rPE-based bio-composites.

Coefficient of thermal expansion ($\text{ppm} \times \text{K}^{-1}$)													
T (°C)	rPE-NF			rPE-CNF			rPE-CNF_MA			rPE-CNF_MA			
	rPE	10	20	30	50	10	20	30	50	10	20	30	50
40	-101.35	-98.6	-53.37	-23.77	-16.13	-47.37	-67.08	-56.29	-72.85	-71.75	-47.31	-25.32	14.7
50	-147.80	-53.93	-75.89	-20.26	-34.98	-125.6	-78.29	-105.65	-9.97	-109.54	-91.3	-55.3	7.07
60	-162.37	-68.04	-60.03	-16.2	-45.83	-65.88	-51.17	-64.78	19.82	-87.88	-107.89	-104.81	9.78
70	-179.34	-93.12	-75.42	-17.59	-60.46	-58.86	-40.92	-55.14	33.08	-84.49	-119.35	-33.32	16.6
80	-237.38	-132.61	-118.46	-30.38	-84.14	-71.03	-25.64	-46.65	39.98	-123.31	-140.73	-53.0	34.61
90	-320.66	-205	-201.68	-42.53	-101.11	-119.63	-56.55	-46.77	34.69	-213.58	-185.73	-110.53	34.52
100	-392.55	-332.3	-317.14	-246.22	-110.97	-347.07	-140.31	-116.88	-84.93	-443.68	-229.85	-195.62	-55.99
110	-973.62	-260.5	-366.86	-177.3	-88.66	-365.81	-263.1	-187.76	-173.37	-375.77	-189.65	-198.37	-147.81

Abbreviations: CNF, cellulosic nanofiber; MA, maleic anhydride; NF, nanofiber; rPE, recycled-polyethylene.

composite materials when cellulosic nanofiber increases.⁶⁷ In another study, the additive ratio increases in the composite materials produced with wood cellulose and PP, the free mobility is limited, and the viscosity values increase.⁶⁸ However, the most negligible reduction was less in MA-modified cellulose fibers than in NF and CNF, suggesting that MA forms a more compatible interface with the polymer matrix. The higher the cellulose fiber content results, the higher the melt viscosity of the composite.

Moreover, shear, compression, and elongation stress by the molten composite and their degradation and fiber breakage result in observed MFI increases. Especially in NF and CNF-based composites, fiber breakage was also observed from SEM micrographs (Figure 9). It showed that after the MA modification, the fibers were better embedded in the polymer matrix than raw hemp fibers and cellulosic nanofibers, there was a better interface between the matrix and the reinforcement material after the modification process, and an effective charge transfer took place.⁶⁹ Figure 9 shows typical SEM photographs of fractured surfaces of recycled polyethylene/cellulose fiber composites. Good interaction and good fiber dispersion in the matrix are the most important factors for mechanical properties. Fracture surface examination with SEM provides information about the fiber/matrix interphase. Sections marked with circles in the SEM micrograph show regions where fibers tend to agglomerate and break. In the interfacial images of the composites containing NF and CNF fibers, the gaps formed between the fiber/matrix and confirming the poor adhesion between the reinforcement and the matrix are pretty significant compared to CNF_MA.

3.2.4 | Tensile properties

At least five tests were performed to determine the tensile strength and elasticity of the produced composite materials. The results are given with their SDs. Various factors significantly impact the mechanical performance of natural fiber-reinforced polymer composite materials.⁷⁰ The stress transfer efficiency in cellulosic nanofiber-reinforced composite materials depends on grain size, additive ratios, and surface area.⁷⁰ Figure 10A shows that the increase in the cellulose fiber content generally leads to an increase in the maximum tensile strength values of the composites. However, the rise in CNF fiber content was found to have a much lower effect on composites. The increases in maximum tensile strength of rPE composites were calculated as 30.76% and 11.28% at a 30% loading rate for NF and CNF fibers and 26.6% at a 50% loading rate for CNF_MA fibers. It is observed that the

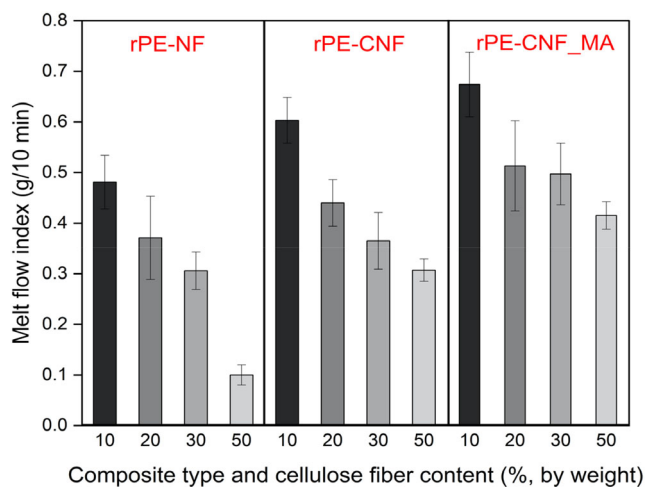


FIGURE 8 Effect of cellulose fiber content on composites' melt flow index (MFI).

tensile values of raw hemp and cellulosic nanofiber composites decrease at 50% fiber loading due to poor fiber-matrix interface and low-stress transfer; this value decreases due to fiber-matrix interface and insufficient stress transfer.⁷¹ However, it can be attributed to the reduced aspect ratio of the fibers due to breakage in the cellulose fibers during processing, as previously seen in SEM micrographs.⁷² On the other hand, the tensile strength of rPE-CNF_MA composites increases as the additive ratio increases, indicating that the MA modification improves the interfacial stress transfer by improving the properties of both phases.

The main reason why the strengths in NFs at up to 50% are higher than CNF and CNF_MA could be attributed to the basic structure of the plant fiber. The polymeric substance is slowly incorporated into the amorphous region of the fiber. The crystal domain contains a significant number of bonds, called strong intramolecular hydrogen bonds, that can form the cellulosic block that increases the challenges for other chemical inputs.⁷³ In this study, NF contains cellulose, hemicellulose and lignin, as well as low amounts of oil, waxes, protein, and different water-soluble components. As seen in XRD analysis, CNF, and CNF_MA crystallinity is high. It has been stated in previous studies that the crystal structure in cellulose inhibits this development.^{74–76} Elongations at break show similar trends for NF, CNF, and CNF_MA fibers (Figure 10B). However, at the same additive ratios, MA-modified fibers always have a slightly higher elongation at break. The main reason for this is that the functional group of MA binds with the OH-groups of Cellulose and provides a good coupling with the polymer matrix material, giving the hydrophilic raw hemp fiber a hydrophobic feature.⁷⁷

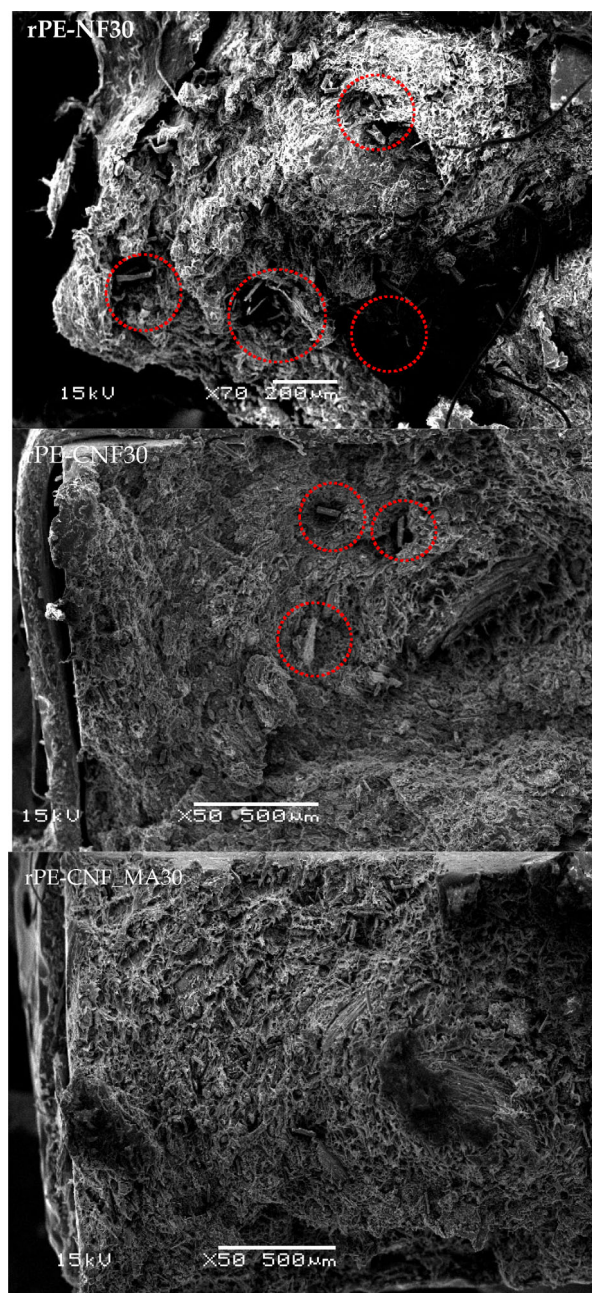


FIGURE 9 Scanning electron microscope (SEM) micrographs of cellulosic fiber/recycled polyethylene composites containing a 30 wt% of cellulose fibers (70 \times and 50 \times , 50 \times magnification respectively).

For all cellulose samples, an increase in cellulose content contributes to an increase in the elastic modulus of the composites (Figure 10C). Composites with higher fiber content offer higher stiffness as the fibers restrict the mobility of polymer macromolecules when subjected to tensile stress. With the addition of NF, CNF, and CNF_MA reinforcements, a significant increase was observed in Young's modulus values of the composite material, especially after the additive ratio of 30% by

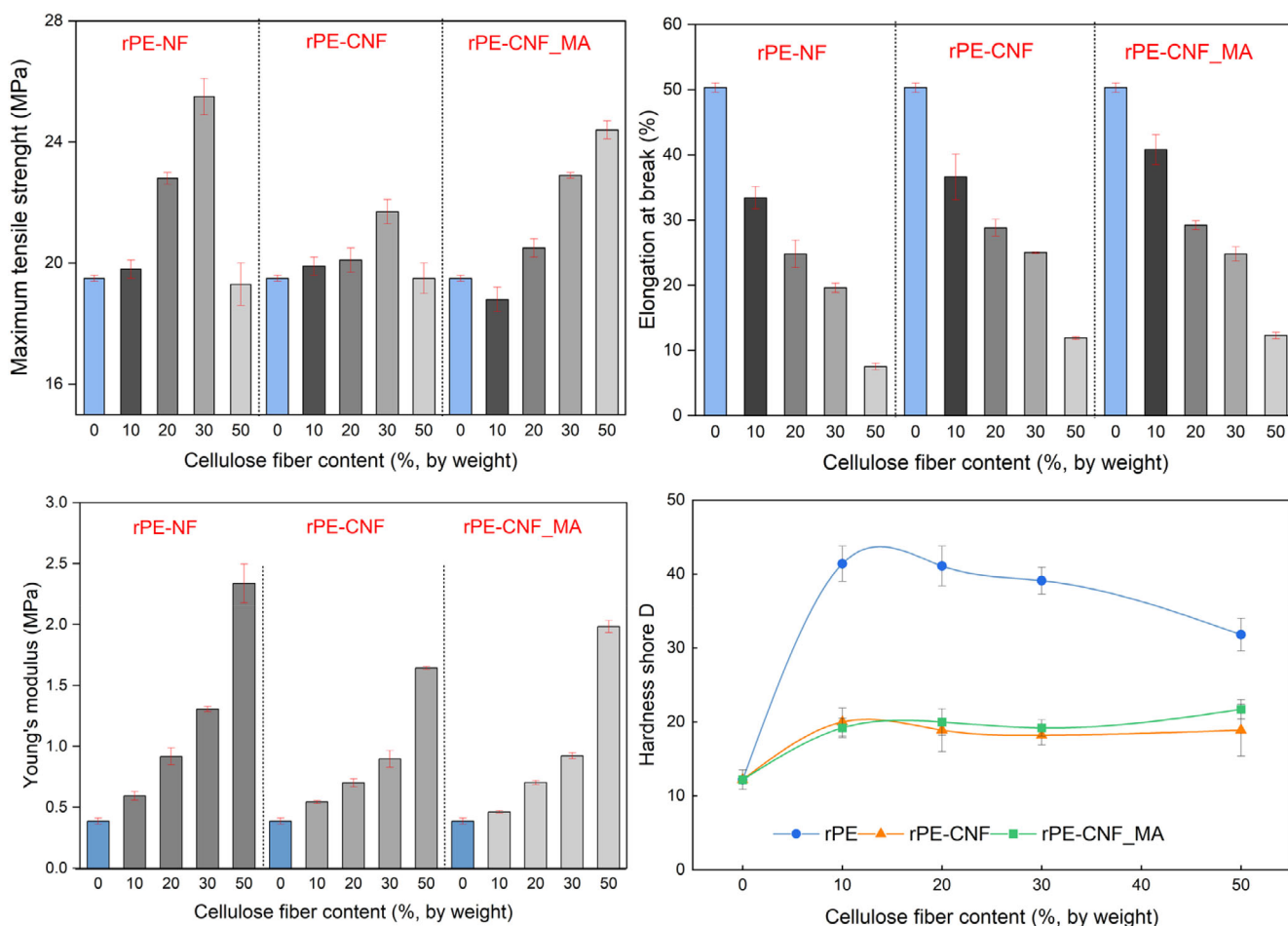


FIGURE 10 Effect of cellulose fiber content and modification agent on (A) the maximum tensile strength of the composite, (B) elongation at break of composites at the maximum tensile strength, (C) modulus of elasticity, and (D) hardness of composite.

weight. When this value is evaluated with tensile strength and elongation at break, MA-modified fibers significantly improve the mechanical properties.

At least 10 measurements were taken from each composite to determine the shore hardness of the produced composite materials. The results are given with their SDs. The Shore *D* hardness indicates the hardness value of the polymer matrix composite material. The hardness of the composite materials produced with 10%–50% fiber reinforcement (NF, CNF, CNF_MA) shows a significant change compared to the blank rPE material (Figure 10D). The Shore *D* hardness values of raw hemp tend to decrease as the fiber additive ratio increases. The main reason is that the polymer matrix cannot bond sufficiently with the hemp fibers. However, CNF and CNF_MA fibers provide rigidity and strength to the structure due to their interaction and the strong hydrogen bonds that hold the fibers together.

On the other hand, the mass ratio of CNF and CNF_MA fibers did not significantly change the stiffness. At the highest additive ratios, the hardness of rPE

increased by 55% in the rPE-CNF composite, while it increased by 78% in the rPE-CNF_MA composite. These results show that chemical extraction and surface modification treatments applied to raw hemp are beneficial in improving the mechanical properties of recycled polyethylene even when used at the lowest additive ratio.

Table 2 summarizes the mechanical properties of various natural fiber-reinforced recycled polyethylene and pure polyethylene matrix composite materials. In general, it was observed that the composites produced with recycled polyethylene showed mechanical properties close to those produced with pure polyethylene. In this study, it was observed that the strength of surface-treated composites decreased at the same filling ratios compared to natural hemp fibers. However, modified with MA composites increased the strength compared to surface treatment samples. The mechanical properties of natural filler composites depend on many factors. Size and size distribution, fill rates, orientation etc. it could be. The results all show that the addition of hemp fibers improves the load bearing capacity of the composites. Similar observations

TABLE 2 Comparison of mechanical properties of raw fiber reinforced-PE based composites.

Filler	Polymer	Filler (%)	Tensile strength (MPa)	Elasticity	Elongation at break (%)	Refs.
Sisal	RC-HDPE	0	20.72 ± 0.5	No data	No data	78
		1	20.66 ± 0.9			
		2	20.41 ± 1.1			
		4	20.30 ± 1.0			
Rice-husk	RC-HDPE	0	26.0 ± 0.5	No data	No data	79
		50	25.1 ± 2.9			
Raw salago	HDPE	0	28.34	No data	No data	80
		10	22.335			
		20	19.59			
		30	15.875			
Modified-salago	HDPE	0	28.34	No data	No data	
		10	26.855			
		20	26.25			
		30	26.01			
Peanut shell powder	RC-PP/PE	0	22.5	53.1	No data	81
		5	19.8	53.2		
		10	22.5	76.5		
		15	22.5	77.1		
		20	27.5	77.2		
		25	18	77.3		
Raw hemp	RC-HDPE	0	19.1	No data	17.9	82
		20	18.6		7	
		30	45.7		3.7	
		40	60.2		3	
Modified hemp		0	19.1	No data	17.9	
		20	15.7		4.5	
		30	27.4		5.4	
		40	26		3.3	
Banana peel powder	Waste LDPE	0	22	0.5	No data	83
		5	21.8	0.6		
		10	23	1.5		
		15	49	2.55		
		20	40	2		
		25	39	2.1		
NF	rPE	0	19.5 ± 0.1	0.4 ± 0.025	50.3 ± 0.7	This study
		10	19.8 ± 0.5	0.6 ± 0.035	33.4 ± 1.7	
		20	22.8 ± 0.6	0.9 ± 0.07	24.8 ± 2.1	
		30	25.5 ± 0.9	1.3 ± 0.02	19.6 ± 0.7	
		50	19.3 ± 1.1	2.3 ± 0.16	7.5 ± 0.5	
CNF		0	19.5 ± 0.1	0.4 ± 0.025	50.3 ± 0.7	
		10	19.9 ± 0.7	0.5 ± 0.013	36.6 ± 3.5	
		20	20.1 ± 0.5	0.7 ± 0.032	28.8 ± 1.3	
		30	21.7 ± 0.5	0.9 ± 0.07	25 ± 0.1	

(Continues)

TABLE 2 (Continued)

Filler	Polymer	Filler (%)	Tensile strength (MPa)	Elasticity	Elongation at break (%)	Refs.
CNF_MA		50	19.5 ± 0.7	1.6 ± 0.012	11.9 ± 0.2	
		0	19.5 ± 0.1	0.4 ± 0.025	50.3 ± 0.7	
		10	18.8 ± 0.4	0.5 ± 0.01	40.8 ± 2.3	
		20	20.5 ± 0.5	0.7 ± 0.02	29.2 ± 0.7	
		30	22.9 ± 0.1	0.9 ± 0.025	24.8 ± 1.1	
		50	24.4 ± 0.3	2 ± 0.05	12.3 ± 0.5	

Abbreviations: CNF, cellulosic nanofiber; LDPE, low-density polyethylene; MA, maleic anhydride; NF, nanofiber; PE, polyethylene; PP, polypropylene; RC-HDPE, recycled-high density polyethylene; rPE, recycled-polyethylene.

for other filler-reinforced polymer composites are reported by Vázquez et al.⁸⁴ In addition, the developed composites are less deformed up to the maximum load, which provides lower elongation. The modification studies observed that the composites produced with surface-modified fibers with MA exhibited better mechanical properties than raw fibers. The main reason for this is that MA reduces the surface tension of rPE and thus increases its miscibility with the filler. This result shows that MA is a valid modification for all cellulosic or non-cellulosic applications.^{85,86}

As a result, it was evaluated that instead of materials produced with pure polyethylene, composites prepared with natural fiber reinforcements of waste and recycled polyethylene could be used industrially.

3.2.5 | Water absorption

In all three types of fillers, the percentage of water absorption increased as the additive ratio increased (Figure 11). However, in the 10% and 30% additive ratios, the water absorption capacity values are pretty close, while the increase is relatively high compared to rPE at 50% additive ratios. The water absorption capacity of the rPE-NF, rPE-CNF, and rPE-CNF_MA composite types increased by 597%, 450%, and 160%, respectively. It has been reported that cellulose and hemicelluloses are primarily responsible for the high-water absorption in organic fillers.^{87–89} The higher the filler content, the higher the Cellulose and, therefore, the higher the water absorption.⁹⁰ The increase in the amount of water absorption in the raw hemp fiber with an additive rate of 50% is attributed to the lignocellulosic structure of the hemp fiber.¹⁸ The lignocellulosic structure has highly polar compounds, and therefore, the water affinity of hemp fiber is high.⁸² Since the extraction process removed hydrophilic compounds from the raw hemp fiber, a 47.5% decrease was observed in the water

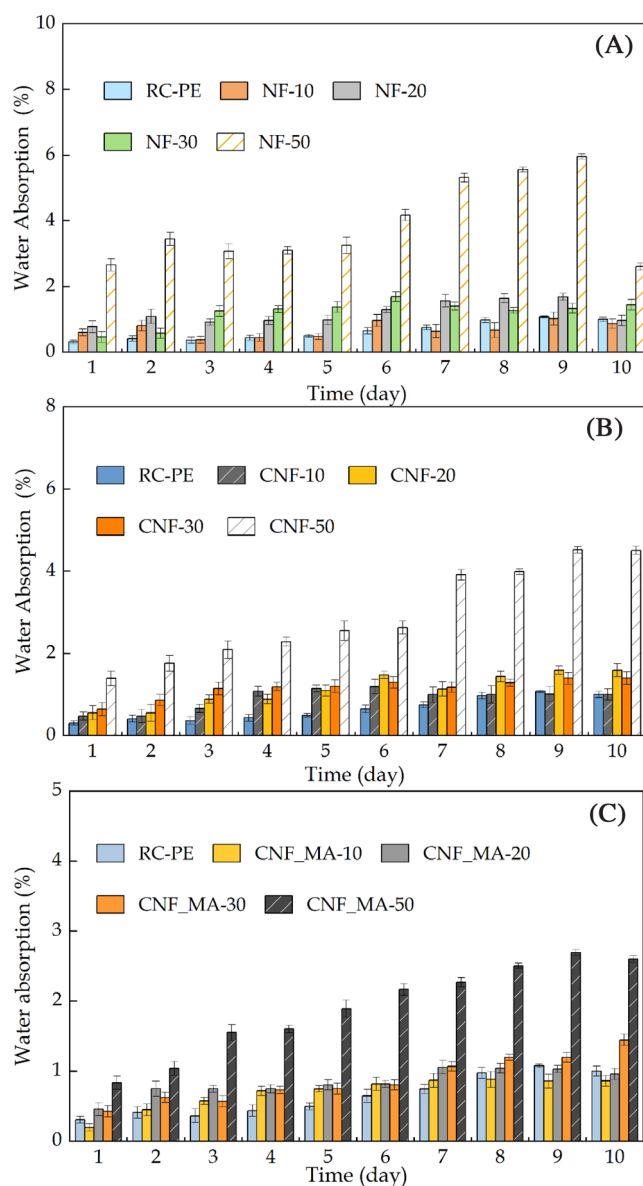


FIGURE 11 Swelling properties of recycled-polyethylene (rPE), rPE-nanofiber (NF), rPE-CNF, and rPE-CNF_MA biocomposites.

absorption capacity of the rPE-CNF composites when the highest additive rates were evaluated compared to the raw hemp-reinforced composite (Figure 11A,B). Similarly, by improving the polymer and reinforcement material interface with MA modification, a 68% decrease was determined in the water absorption capacity compared to the raw hemp-reinforced composite (Figure 11C). Despite the higher water uptake noticeable with the increase in filler content, the materials are still considered durable engineering materials according to literature values reported by Alomayri et al.⁹¹

4 | CONCLUSION

In this study, it has been determined that surface modification can be used to improve the properties, durability and wettability of hemp fibers and that the interfacial bond between the matrix and the fibers can be changed, albeit limited. Therefore, it can be considered as an appropriate method for composite materials where hemp fibers and waste polymers can be used as binders. In the SEM and FTIR analyses, it was determined that both cellulose extraction and modification with MA were performed successfully and it was shown that it can be successfully applied in cellulose-containing plant species such as hemp.

The most important part of this study is the analysis of the composite material produced with waste polyethylene and their mechanical properties. It was determined that the Shore hardness and water absorption values changed proportionally with the additive ratios. MFI results are also instructive in determining the process parameters to produce composites in future studies. Although the mechanical strength of the produced composite materials may seem negative at first glance, it actually contains very important results. When the tensile strength results are carried out, it could be seems NF without any modification can provide strength up to 25 MPa. Only 21 MPa can be reached with composite materials containing cellulose. Therefore, it is not reasonable to obtain pure cellulose as a result of long processes and to produce composite materials from it, as it brings low strength values. However, the maximum strength value with 30% filling ratio in NF composites increased up to 50% filling ratio with Maleic Anhydride modification. This result plays a key role for the study and showed that the modification was successful in improving the filler and binder interface, and even higher filler ratios could be studied. In addition, it is obvious that 50% filling rates can be easily exceeded by working with different molding temperatures, times and pressures for the production of composite materials. It is clear that all

mechanical and structural properties of modified fiber surface are significantly affected by the chemical treatment of hemp fibers. As a result of, the application and diversification of these modifications to different bio based materials and various binders is possible to expand the applicability of not only hemp fibers but also bio based materials and waste polymers in high-end applications.

ACKNOWLEDGMENTS

The authors gratefully thank to Kırıkkale University Research Fund for financial support for this Project, numbered 2021/021.

DATA AVAILABILITY STATEMENT

Data will be submit if they require.

ORCID

İbrahim Bilici  <https://orcid.org/0000-0001-8151-6911>

Ayşegül Ülkü Metin  <https://orcid.org/0000-0001-8494-601X>

REFERENCES

1. Zhao X, Copenhaver K, Wang L, et al. Recycling of natural fiber composites: challenges and opportunities. *Resour Conserv Recycl.* 2022;177:105962. doi:10.1016/j.resconrec.2021.105962
2. Owen MM, Achukwu EO, Romli AZ, Md Akil H. Recent advances on improving the mechanical and thermal properties of kenaf fibers/engineering thermoplastic composites using novel coating techniques: a review. *Compos Interfaces.* 2023;1–27:1–27. doi:10.1080/09276440.2023.2179238
3. Owen MM, Achukwu EO, Hazizan AM, Romli AZ, Ishiaku US. Characterization of recycled and virgin polyethylene terephthalate composites reinforced with modified kenaf fibers for automotive application. *Polym Compos.* 2022;43(11):7724–7738. doi:10.1002/pc.26866
4. Stelea L, Filip I, Lisa G, et al. Characterisation of hemp fibres reinforced composites using thermoplastic polymers as matrices. *Polymers.* 2022;14(3):481. doi:10.3390/polym14030481
5. Felix Sahayaraj A, Muthukrishnan M, Ramesh M. Experimental investigation on physical, mechanical, and thermal properties of jute and hemp fibers reinforced hybrid polylactic acid composites. *Polym Compos.* 2022;43(5):2854–2863. doi:10.1002/pc.26581
6. Liao J, Zhang S, Tang X. Sound absorption of hemp fibers (*Cannabis sativa L.*) based nonwoven fabrics and composites: a review. *J Nat Fibers.* 2020;19(4):1297–1309. doi:10.1080/15440478.2020.1764453
7. Fico D, Rizzo D, Casciaro R, Esposito Corcione C. A review of polymer-based materials for fused filament fabrication (FFF): focus on sustainability and recycled materials. *Polymers.* 2022; 14(3):465. doi:10.3390/polym14030465
8. Andrew JJ, Dhakal HN. Sustainable biobased composites for advanced applications: recent trends and future opportunities – a critical review. *Compos C: Open Access.* 2022;7:100220. doi:10.1016/j.jcomc.2021.100220
9. Sala B, Watjanatepin P, Zarafshani H, et al. Creep behaviour of eco-friendly sandwich composite materials under hygrothermal conditions. *Compos B: Eng.* 2022;247:110291. doi:10.1016/j.compositesb.2022.110291

10. Burgada F, Fages E, Quiles-Carrillo L, et al. Upgrading recycled polypropylene from textile wastes in wood plastic composites with short hemp fiber. *Polymers*. 2021;13(8):1248. doi:10.3390/polym13081248
11. Weiss M, Haufe J, Carus M, et al. A review of the environmental impacts of biobased materials. *J Ind Ecol*. 2012;16:169-181. doi:10.1111/j.1530-9290.2012.00468.x
12. La Rosa AD, Recca G, Summerscales J, Latteri A, Cozzo G, Cicala G. Bio-based versus traditional polymer composites, a life cycle assessment perspective. *J Clean Prod*. 2014;74:135-144. doi:10.1016/j.jclepro.2014.03.017
13. Adesina I, Bhowmik A, Sharma H, Shahbazi A. A review on the current state of knowledge of growing conditions, agronomic soil health practices and utilities of hemp in the United States. *Agri*. 2020;10(4):129. doi:10.3390/agriculture10040129
14. Bourmaud A, Baley C. Investigations on the recycling of hemp and sisal fibre reinforced polypropylene composites. *Polym Degrad Stab*. 2007;92(6):1034-1045. doi:10.1016/j.polymdegradstab.2007.02.018
15. Awais H, Nawab Y, Anjang A, Md Akil H, Zainol Abidin MS. Effect of fabric architecture on the shear and impact properties of natural fibre reinforced composites. *Compos B: Eng*. 2020;195:108069. doi:10.1016/j.compositesb.2020.108069
16. Li M, Pu Y, Thomas VM, et al. Recent advancements of plant-based natural fiber-reinforced composites and their applications. *Compos B: Eng*. 2020;200:108254. doi:10.1016/j.compositesb.2020.108254
17. Dolza C, Gongga E, Fages E, Tejada-Oliveros R, Balart R, Quiles-Carrillo L. Green composites from partially bio-based poly (butylene succinate-co-adipate)-pbsa and short hemp fibers with itaconic acid-derived compatibilizers and plasticizers. *Polymers*. 2022;14(10):1968. doi:10.3390/polym14101968
18. Dolça C, Fages E, Gongga E, Garcia-Sanoguera D, Balart R, Quiles-Carrillo L. The effect of varying the amount of short hemp fibers on mechanical and thermal properties of wood-plastic composites from biobased polyethylene processed by injection molding. *Polymers*. 2021;14(1):138. doi:10.3390/polym14010138
19. Mohanavel V, Sathish T, Ravichandran M, Ganeshan P, Ravi Kumar MM, Subbiah R. Experimental investigations on mechanical properties of cotton/hemp fiber reinforced epoxy resin hybrid composites. *J Phys Conf Ser*. 2021;2027(1):012015. doi:10.1088/1742-6596/2027/1/012015
20. Asthana A, Srivastava V. Mechanical behavior of silk/hemp-steel wool – epoxy composite. *Mater Today: Proc*. 2021;44(1):2228-2231. doi:10.1016/j.matpr.2020.12.358
21. Antony S, Cherouat A, Montay G. Effect of fibre content on the mechanical properties of hemp fibre woven fabrics/polypropylene composite laminates. *Polym Polym Compos*. 2021;29(9S):790-802. doi:10.1177/09673911211023942
22. Boccarusso L, De Fazio D, Durante M. Production of PP composites reinforced with flax and hemp woven mesh fabrics via compression molding. *Inventions*. 2021;7(1):5. doi:10.3390/inventions7010005
23. Achukwu EO, Owen MM, Danladi A, et al. Effect of glass fiber loading and reprocessing cycles on the mechanical, thermal, and morphological properties of isotactic polypropylene composites. *J Appl Polym Sci*. 2023;140(10):16. doi:10.1002/app.53588
24. Gupta A, Chudasama B, Chang BP, Mekonnen T. Robust and sustainable pbat – hemp residue biocomposites: reactive extrusion compatibilization and fabrication. *Compos Sci Technol*. 2021;215:109014. doi:10.1016/j.compscitech.2021.109014
25. Laqraa C, Ferreira M, Soulat D, Labanieh A-R. Natural fibre composites manufacture using wrapped hemp roving with PA11. *Mater Circ Econ*. 2022;4(17):9. doi:10.1007/s42824-022-00057-3
26. Panaitescu DM, Vuluga Z, Ghiurea M, Iorga M, Nicolae C, Gabor R. Influence of compatibilizing system on morphology, thermal and mechanical properties of high flow polypropylene reinforced with short hemp fibers. *Compos B: Eng*. 2015;69:286-295. doi:10.1016/j.compositesb.2014.10.010
27. Liu M, Silva DA, Fernando D, et al. Controlled retting of hemp fibres: effect of hydrothermal pre-treatment and enzymatic retting on the mechanical properties of unidirectional hemp/epoxy composites. *Compos Part A: Appl Sci Manuf*. 2016;88:253-262. doi:10.1016/j.compositesa.2016.06.003
28. Kolářová K, Vosmanská V, Rimpelová S, Švorčík V. Effect of plasma treatment on cellulose fiber. *Cellulose*. 2013;20(2):953-961. doi:10.1007/s10570-013-9863-0
29. Wang HM, Postle R, Kessler RW, Kessler W. Removing pectin and lignin during chemical processing of hemp for textile applications. *Text Res J*. 2003;73(8):664-669. doi:10.1177/004051750307300802
30. Sepe R, Bollino F, Boccarusso L, Caputo F. Influence of chemical treatments on mechanical properties of hemp fiber reinforced composites. *Compos B: Eng*. 2018;133:210-217. doi:10.1016/j.compositesb.2017.09.030
31. Owen MM, Ishiaku US, Danladi A, Dauda BM, Romli AZ. Mechanical properties of epoxy-coated sodium hydroxide and silane treated kenaf/recycled polyethylene TEREPH-thalate (RPET) composites: effect of chemical treatment. *AIP Conf Proc*. 2018;1985:030001. doi:10.1063/1.5047159
32. Georgiopoulou I, Pappa GD, Vouyiouka SN, Magoulas K. Recycling of post-consumer multilayer Tetra Pak® packaging with the selective dissolution-precipitation process. *Resour Conserv Recycl*. 2021;165:105268. doi:10.1016/j.resconrec.2020.105268
33. Kan M, Miller SA. Environmental impacts of plastic packaging of food products. *Resour Conserv Recycl*. 2022;180:106156. doi:10.1016/j.resconrec.2022.106156
34. Nguyen LK, Na S, Hsuan YG, Spataro S. Uncertainty in the life cycle greenhouse gas emissions and costs of HDPE PIPE alternatives. *Resour Conserv Recycl*. 2020;154:104602. doi:10.1016/j.resconrec.2019.104602
35. Gao H, Liu Q, Yan C, et al. Macro-and/or microplastics as an emerging threat effect crop growth and soil health. *Resour Conserv Recycl*. 2022;186:106549. doi:10.1016/j.resconrec.2022.106549
36. Başaran Kankılıç G, Metin AÜ. Phragmites australis as a new cellulose source: extraction, characterization, and adsorption of methylene blue. *J Mol Liq*. 2020;312:113313. doi:10.1016/j.molliq.2020.113313
37. Nascimento SA, Rezende CA. Combined approaches to obtain cellulose nanocrystals, nanofibrils and fermentable sugars from elephant grass. *Carbohydr Polym*. 2018;180:38-45. doi:10.1016/j.carbpol.2017.09.099
38. Ndwandwa N, Iwarere SA, Daramola MO, Ayaa F, Kirabira JB. Extraction and characterization of cellulose nanofibers from yellow thatching grass (*Hyparrhenia filipendula*) straws via acid hydrolysis. *Waste Biomass Valorization*. 2023;1-10. doi:10.1007/s12649-022-02014-2

39. Radakisnin R, Abdul Majid MS, Jamir MR, Jawaid M, Sultan MT, Mat Tahir MF. Structural, morphological and thermal properties of cellulose nanofibers from Napier fiber (*Pennisetum purpureum*). *Materials*. 2020;13(18):4125. doi:10.3390/ma13184125
40. Kian LK, Saba N, Jawaid M, Alothman OY, Fouad H. Properties and characteristics of nanocrystalline cellulose isolated from olive fiber. *Carbohydr Polym*. 2020;241:116423. doi:10.1016/j.carbpol.2020.116423
41. Chen M, Chen C, Liu C, Sun R. Homogeneous modification of sugarcane bagasse with maleic anhydride in 1-butyl-3-methylimidazolium chloride without any catalysts. *Ind Crops Prod*. 2013;46:380-385. doi:10.1016/j.indcrop.2013.02.023
42. Li J, Wei X, Wang Q, et al. Homogeneous isolation of nanocellulose from sugarcane bagasse by high pressure homogenization. *Carbohydr Polym*. 2012;90(4):1609-1613. doi:10.1016/j.carbpol.2012.07.038
43. Nam S, French AD, Condon BD, Concha M. Segal crystallinity index revisited by the simulation of X-ray diffraction patterns of cotton cellulose I β and cellulose II. *Carbohydr Polym*. 2016; 135:1-9. doi:10.1016/j.carbpol.2015.08.035
44. Klemm D, Heublein B, Fink H-P, Bohn A. Cellulose: fascinating biopolymer and sustainable raw material. *Angew Chem Int ed*. 2005;44(22):3358-3393. doi:10.1002/anie.200460587
45. Feng Y-H, Cheng T-Y, Yang W-G, et al. Characteristics and environmentally friendly extraction of cellulose nanofibrils from sugarcane bagasse. *Ind Crops Prod*. 2018;111:285-291. doi:10.1016/j.indcrop.2017.10.041
46. Singh S, Cheng G, Sathitsuksanoh N, et al. Comparison of different biomass pretreatment techniques and their impact on chemistry and structure. *Front Energy Res*. 2015;2(62):12. doi:10.3389/fenrg.2014.00062
47. Bulut Y, Erdoğlan ÜH. Selüloz Esaslı Doğal Liflerin Kompozit Üretiminde Takviye Materyali Olarak Kullanımı. *J Text*. 2011; 82:26-35.
48. Mohanty AK, Misra M, Hinrichsen G. Biofibres, biodegradable polymers and biocomposites. *Macromol Mater Eng*. 2000;276-277: 1-24. doi:10.1002/(SICI)1439-2054(20000301)276:1<1::AID-MAME1>3.0.CO;2-W
49. Kaya S. *Geri Dönüşüm İplikçığının Kenevir Lifi Kullanımın Araştırılması. Yüksek Lisans Tezi*. Uşak Üniversitesi, Fen Bilimleri Enstitüsü, Uşak; 2021.
50. Johar N, Ahmad I, Dufresne A. Extraction, preparation and characterization of cellulose fibres and nanocrystals from rice husk. *Ind Crops Prod*. 2012;37(1):93-99. doi:10.1016/j.indcrop.2011.12.016
51. Martins MA, Teixeira EM, Corrêa AC, Ferreira M, Mattoso LH. Extraction and characterization of cellulose whiskers from commercial cotton fibers. *J Mater Sci*. 2011;46(24):7858-7864. doi:10.1007/s10853-011-5767-2
52. Chirayil CJ, Joy J, Mathew L, Mozetic M, Koetz J, Thomas S. Isolation and characterization of cellulose nanofibrils from *Helicteres Isora* plant. *Ind Crops Prod*. 2014;59:27-34. doi:10.1016/j.indcrop.2014.04.020
53. Owen MM, Achukwu EO, Shuib SB, Ahmad ZR, Abdullah AH, Ishiaku US. Effects of high-temperature optimization and resin coating treatment on the mechanical, thermal, and morphological properties of natural kenaf fiber-filled engineering plastic composites. *Polym Compos*. 2023;44(4):2512-2529. doi:10.1002/pc.27260
54. Owen MM, Achukwu EO, Akil HM, et al. Effect of epoxy concentrations on thermo-mechanical properties of kenaf fiber – recycled poly (ethylene terephthalate) composites. *J Ind Text*. 2022;52:152808372211274. doi:10.1177/15280837221127441
55. Ventura-Cruz S, Tecante A. Extraction and characterization of cellulose nanofibers from rose stems (*Rosa* spp.). *Carbohydr Polym*. 2019;220:53-59. doi:10.1016/j.carbpol.2019.05.053
56. Li Y, Xiao H, Chen M, Song Z, Zhao Y. Absorbents based on maleic anhydride-modified cellulose fibers/diatomite for dye removal. *J Mater Sci*. 2014;49(19):6696-6704. doi:10.1007/s10853-014-8270-8
57. Zhou Y, Jin Q, Hu X, Zhang Q, Ma T. Heavy metal ions and organic dyes removal from water by cellulose modified with maleic anhydride. *J Mater Sci*. 2012;47(12):5019-5029. doi:10.1007/s10853-012-6378-2
58. Owen MM, Ishiaku US, Danladi A, Dauda BM, Romli AZ. The effect of surface coating and fibre loading on thermo-mechanical properties of recycled polyethylene terephthalate (RPET)/epoxy-coated kenaf fibre composites. *AIP Conf Proc*. 2018;1985:030002. doi:10.1063/1.5047160
59. Yang H, Yan R, Chen H, Lee DH, Zheng C. Characteristics of hemicellulose, cellulose and lignin pyrolysis. *Fuel*. 2007;86(12-13):1781-1788. doi:10.1016/j.fuel.2006.12.013
60. Morán JI, Alvarez VA, Cyras VP, Vázquez A. Extraction of cellulose and preparation of nanocellulose from sisal fibers. *Cellulose*. 2007;15(1):149-159. doi:10.1007/s10570-007-9145-9
61. Kargarzadeh H, Ahmad I, Abdullah I, Dufresne A, Zainudin SY, Sheltami RM. Effects of hydrolysis conditions on the morphology, crystallinity, and thermal stability of cellulose nanocrystals extracted from kenaf bast fibers. *Cellulose*. 2012; 19(3):855-866. doi:10.1007/s10570-012-9684-6
62. Poletto M, Ornaghi H, Zattera A. Native cellulose: structure, characterization and thermal properties. *Materials*. 2014;7(9): 6105-6119. doi:10.3390/ma7096105
63. Cichosz S, Masek A, Wolski K, Zaborski M. Universal approach of cellulose fibres chemical modification result analysis via commonly used techniques. *Polym Bull*. 2018;76(5):2147-2162. doi:10.1007/s00289-018-2487-7
64. Luyt AS, Molefi JA, Krump H. Thermal, mechanical and electrical properties of copper powder filled low-density and linear low-density polyethylene composites. *Polym Degrad Stab*. 2006;91(7):1629-1636. doi:10.1016/j.polymdegradstab.2005.09.014
65. Izwan SM, Sapuan SM, Zuhri MYM, Mohamed AR. Thermal stability and dynamic mechanical analysis of benzoylation treated sugar palm/kenaf fiber reinforced polypropylene hybrid composites. *Polymers*. 2021;13(17):2961. doi:10.3390/polym13172961
66. Carvalho MS, Azevedo JB, Barbosa JD. Effect of the melt flow index of an HDPE matrix on the properties of composites with wood particles. *Polym Test*. 2020;90:106678. doi:10.1016/j.polymertesting.2020.106678
67. Alidadi-Shamsabadi M, Behzad T, Bagheri R, Nari-Nasrabadi B. Preparation and characterization of Low-density polyethylene/thermoplastic starch composites reinforced by cellulose nanofibers. *Polym Compos*. 2014;36(12):2309-2316. doi:10.1002/pc.23144

68. Kumari R, Ito H, Takatani M, Uchiyama M, Okamoto T. Fundamental studies on wood/cellulose-plastic composites: effects of composition and cellulose dimension on the properties of cellulose/PP composite. *J Wood Sci.* 2007;53(6):470-480. doi:10.1007/s10086-007-0889-5
69. Roumeli E, Terzopoulou Z, Pavlidou E, et al. Effect of maleic anhydride on the mechanical and thermal properties of hemp/high-density polyethylene green composites. *J Therm Anal Calorim.* 2015;121(1):93-105. doi:10.1007/s10973-015-4596-y
70. Sider I, Nassar MM. Chemical treatment of bio-derived industrial waste filled recycled low-density polyethylene: a comparative evaluation. *Polymers.* 2021;13(16):2682. doi:10.3390/polym13162682
71. Negawo TA, Polat Y, Kilic A. Effect of compatibilizer and fiber loading on ensete fiber-reinforced HDPE green composites: physical, mechanical, and morphological properties. *Compos Sci Technol.* 2021;213:108937. doi:10.1016/j.compscitech.2021.108937
72. Fonseca-Valero C, Ochoa-Mendoza A, Arranz-Andrés J, González-Sánchez C. Mechanical recycling and composition effects on the properties and structure of hardwood cellulose-reinforced high density polyethylene eco-composites. *Compos Part A: Appl Sci Manuf.* 2015;69:94-104. doi:10.1016/j.compositesa.2014.11.009
73. Mahmud S, Hasan KM, Jahid MA, Mohiuddin K, Zhang R, Zhu J. Comprehensive review on plant fiber-reinforced polymeric biocomposites. *J Mater Sci.* 2021;56(12):7231-7264. doi:10.1007/s10853-021-05774-9
74. Mwaikambo LY, Ansell MP. Chemical modification of hemp, sisal, jute, and kapok fibers by alkalization. *J Appl Polym Sci.* 2002;84(12):2222-2234. doi:10.1002/app.10460
75. Abdelmouleh M, Boufi S, Belgacem M, Dufresne A. Short natural-fibre reinforced polyethylene and natural rubber composites: effect of silane coupling agents and fibres loading. *Compos Sci Technol.* 2007;67(7-8):1627-1639. doi:10.1016/j.compscitech.2006.07.003
76. Madsen B. *Properties of Plant Fiber Yarn Polymer Composites: An Experimental Study.* Technical University of Denmark; 2004 BYG-Rapport No. R-082.
77. Sullins T, Pillay S, Komus A, Ning H. Hemp fiber reinforced polypropylene composites: the effects of material treatments. *Compos B: Eng.* 2017;114:15-22. doi:10.1016/j.compositesb.2017.02.001
78. Chianelli-Junior R, Reis JML, Cardoso JL, Castro PF. Mechanical characterization of sisal fiber-reinforced recycled HDPE composites. *Mater Res.* 2013;16(6):1393-1397. doi:10.1590/s1516-14392013005000128
79. Orji BO, McDonald AG. Evaluation of the mechanical, thermal and rheological properties of recycled polyolefins rice-hull composites. *Materials.* 2020;13(3):667. doi:10.3390/ma13030667
80. Pouriman M, Dahresobh A, Moradipour M, Caparanga AR. Thermal and nondestructive analysis of high-density polyethylene filled with milled salago fiber. *J Appl Polym Sci.* 2019;136(33):47873. doi:10.1002/app.47873
81. McCaffrey Z, Torres L, Flynn S, et al. Recycled polypropylene-polyethylene torrefied almond shell biocomposites. *Ind Crops Prod.* 2018;125(11):425-432. doi:10.1016/j.indcrop.2018.09.012
82. Lu N, Swan RH, Ferguson I. Composition, structure, and mechanical properties of hemp fiber reinforced composite with recycled high-density polyethylene matrix. *J Compos Mater.* 2011;46(16):1915-1924. doi:10.1177/0021998311427778
83. Jacob J, Mamza PA. Mechanical and thermal behavior of plantain peel powder filled recycled polyethylene composites. *Ovidius Univ Ann Chem.* 2021;32(2):114-119. doi:10.2478/auoc-2021-0017
84. Vázquez A, Domínguez VA, Kenny JM. Bagasse fiber-polypropylene based composites. *J Thermoplast Compos Mater.* 1999;12(6):477-497. doi:10.1177/089270579901200604
85. Liang G, Xu J, Bao S, Xu W. Polyethylene/maleic anhydride grafted polyethylene/organic-montmorillonite nanocomposites. I. Preparation, microstructure, and mechanical properties. *J Appl Polym Sci.* 2004;91(6):3974-3980. doi:10.1002/app.13612
86. Ovali S, Sancak E. Investigation of mechanical properties of jute fiber reinforced low density polyethylene composites. *J Nat Fibers.* 2020;19(8):3109-3126. doi:10.1080/15440478.2020.1838999
87. Ab Ghani MH, Ahmad S. The comparison of water absorption analysis between counterrotating and corotating twin-screw extruders with different antioxidants content in wood plastic composites. *Adv Mater Sci Eng.* 2011;2011:1-4. doi:10.1155/2011/406284
88. Sahu P, Gupta MK. Lowering in water absorption capacity and mechanical degradation of sisal/epoxy composite by sodium bicarbonate treatment and PLA coating. *Polym Compos.* 2019;41(2):668-681. doi:10.1002/pc.25397
89. Sorieul M, Dickson A, Hill S, Pearson H. Plant fibre: molecular structure and biomechanical properties, of a complex living material, influencing its deconstruction towards a biobased composite. *Materials.* 2016;9(8):618. doi:10.3390/ma9080618
90. Muñoz E, García-Manrique JA. Water absorption behaviour and its effect on the mechanical properties of flax fibre reinforced bioepoxy composites. *Int J Polym Sci.* 2015;2015:1-10. doi:10.1155/2015/390275
91. Alomayri T, Assaedi H, Shaikh FUA, Low IM. Effect of water absorption on the mechanical properties of cotton fabric-reinforced geopolymer composites. *J Asian Ceramic Soc.* 2014;2(3):223-230. doi:10.1016/j.jascer.2014.05.005

How to cite this article: Güney O, Bilici İ, Doğan D, Metin Ayşegül Ülkü. Mechanical and thermal properties of recycled polyethylene/surface treated hemp fiber bio-composites. *Polym Compos.* 2023;44(8):4976-4992. doi:10.1002/pc.27463